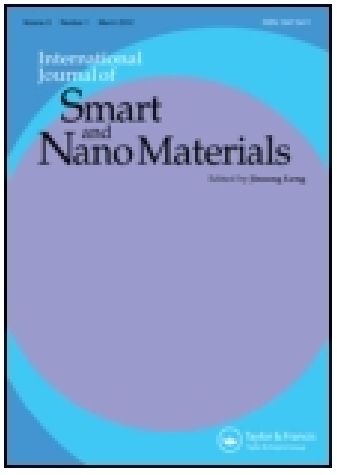

International Journal of Smart and Nano Materials

Publication details, including instructions for authors and subscription information:
http://www.tandfonline.com/loi/tsnm20

A layer-wise MITC9 finite element for the free-vibration analysis of plates with piezo-patches

Maria Cinefra[a], Stefano Valvano[a] & Erasmo Carrera[abc]

[a] Department of Mechanical and Aerospace Engineering, Politecnico di Torino, Torino, Italy

[b] School of Aerospace, Mechanical and Manufacturing Engineering College, RMIT University, Melbourne, Australia

[c] Department of Mathematics, Faculty of Science, King Abdulaziz University, P.O. Box 80203, Jeddah 21589, Saudi Arabia

Published online: 25 Jul 2015.

To cite this article: Maria Cinefra, Stefano Valvano & Erasmo Carrera (2015) A layer-wise MITC9 finite element for the free-vibration analysis of plates with piezo-patches, International Journal of Smart and Nano Materials, 6:2, 85-104, DOI: 10.1080/19475411.2015.1037377

To link to this article: http://dx.doi.org/10.1080/19475411.2015.1037377

International Journal of Smart and Nano Materials, 2015
Vol. 6, No. 2, 85–104, http://dx.doi.org/10.1080/19475411.2015.1037377

Taylor & Francis
Taylor & Francis Group

A layer-wise MITC9 finite element for the free-vibration analysis of plates with piezo-patches

Maria Cinefra[a]*, Stefano Valvano[a] and Erasmo Carrera[a,b,c]

[a]*Department of Mechanical and Aerospace Engineering, Politecnico di Torino, Torino, Italy;* [b]*School of Aerospace, Mechanical and Manufacturing Engineering College, RMIT University, Melbourne, Australia;* [c]*Department of Mathematics, Faculty of Science, King Abdulaziz University, P.O. Box 80203, Jeddah 21589, Saudi Arabia*

(*Received 13 December 2014; final version received 30 March 2015*)

The present article considers the free-vibration analysis of plate structures with piezoelectric patches by means of a plate finite element with variable through-the-thickness layer-wise kinematic. The refined models used are derived from Carrera's Unified Formulation (CUF) and they permit the vibration modes along the thickness to be accurately described. The finite-element method is employed and the plate element implemented has nine nodes, and the mixed interpolation of tensorial component (MITC) method is used to contrast the membrane and shear locking phenomenon. The related governing equations are derived from the principle of virtual displacement, extended to the analysis of electromechanical problems. An isotropic plate with piezoelectric patches is analyzed, with clamped-free boundary conditions and subjected to open- and short-circuit configurations. The results, obtained with different theories, are compared with the higher-order type solutions given in the literature. The conclusion is reached that the plate element based on the CUF is more suitable and efficient compared to the classical models in the study of multilayered structures embedding piezo-patches.

Keywords: plate; patches; finite-element method; piezoelectric materials; mixed interpolated; tensorial components; Carrera's Unified Formulation; layer-wise

1. Introduction

Piezoelectric materials have the ability to convert mechanical energy into electrical energy and vice versa. For the last 50 years, the use of piezoelectric components as electromechanical transducers in sensor as well as in actuator applications has been continuously increasing. More recently, piezoelectrics have been considered to be among the most suitable materials for extending the structural capabilities beyond that of purely passive load-carrying one. Vibration and noise suppression, controlled active deformation, and health monitoring are among the most important applications of these "intelligent" structural components.

Finding analytical solutions for general smart structural problems is a very difficult task, and they only exist for a very few specialized and idealized cases. Meanwhile, the

*Corresponding author. Email: maria.cinefra@polito.it

finite-element (FE) method has become the most widely used technique to model various physical processes, including piezoelectricity. The introduction of piezoelectric material into a passive structure naturally leads to a multilayered component, and it has been recognized that classical models are not suitable for an accurate design of such structures, see for example the review article by Noor and Burton [1] and the references cited herein. The strain induced by the piezoelectric actuators has been used in the works of Crawley and Luis [2], Bailey and Hubbard [3], and Robbins and Reddy [4] as an applied strain that contributes to the total strain of the non-active structure. Interlaminar continuity (IC) of the transverse stresses and the related discontinuity of the slopes of the displacement distributions in thickness direction at the layer interfaces are the main effects arising in multilayered structures which cannot be captured by classical formulations based on love first approximation theories (LFATs) (see e.g. [5]). Many refined theories for plates have been proposed in order to meet the modeling requirements – known as C-requirements – posed by these characteristics; further details can be found in the monograph by Reddy [6] and in the paper by Carrera [7]. For curved structures, Koiter [8] recognized the importance of transverse stress effects even for homogeneous plates and recommended the inclusion of such effects whenever a consistent higher-order model has to be proposed. The fundamentals for the modeling of piezoelectric materials have been given in many contributions, in particular in the pioneering works of Mindlin [9], EerNisse [10], Tiersten and Mindlin [11], and in the monograph by Tiersten [12]. The embedding of piezoelectric layers into plates sharpens the requirements of an accurate modeling of the resulting adaptive structure due to the localized electromechanical coupling, see e.g. the review by Saravanos and Heyliger [13]. Therefore, within the framework of two-dimensional approaches, layer-wise (LW) descriptions have often been proposed, either for the electric field only (see e.g. the works of Kapuria [14] and of Ossadzow-David and Touratier [15]) or for both the mechanical and electrical unknowns (e.g. Heyliger et al. [16]). Ballhause et al. [17] have shown that a fourth-order assumption for the displacements leads to the correct closed-form solution. They conclude that the analysis of local responses requires at least a LW description of the displacements, see also [18]. Benjeddou et al. [19] emphasized that a quadratic electric potential through the plate thickness satisfies the electric charge conservation law exactly. An attempt to mathematically substantiate axiomatic two-dimensional piezoelectric shell formulations by the means of asymptotic expansions can be found in the book by Rogacheva [20]. Zhou et al. (2000) [21] have presented coupled FE models based on a third-order theory for the dynamic response of smart composite plates. In [22] and [23], Arau`jo et al. present a new FE model for the parameter estimation and the analysis of active sandwich laminated plates with a viscoelastic core and laminated anisotropic face layers, as well as piezoelectric sensor and actuator layers. The model is formulated using a mixed LW approach, by considering a higher-order shear deformation theory to represent the displacement field of the viscoelastic core and a first-order shear deformation theory (FSDT) for the displacement field of the adjacent laminated anisotropic face layers and exterior piezoelectric layers. An exhaustive overview of the many different modeling approaches and solution techniques for laminated piezoelectric plates is far beyond the scope of this article; more details on this topic can be found in the already cited review by Saravanos and Heyliger, and in the surveys by Gopinathan et al. [24] and by Benjeddou [25]. Over the last few years, interest has been emerging for mixed formulations also involving stresses and dielectric displacements as primary variables, see for example the recent works of Lammering et al. [26] and of Benjeddou et al. [27]. Some of the most recent contributions to the FE analysis of piezoelectric plates that includes an FSDT description of displacements and a LW form of

the electric potential have been developed by Sheik et al. [28]. The numerical, membrane, and bending behavior of FEs that are based on FSDTs were analyzed by Auricchio et al. [29] in the framework of a suitable variational formulation. The third-order theory of higher-order theories type has been applied by Thornburg and Chattopadhyay [30] to derive FEs that take into consideration electromechanical coupling. Similar elements have more recently been considered by Shu [31]. The extension of the third-order zigzag multilayered theory to finite analysis of electromechanical problems has been proposed by Oh and Cho [32]. An extension to the piezoelectricity of numerically efficient plate elements based on the mixed interpolation of tensorial component (MITC) formulation has recently been provided by Kogl and Bucalem [33,34]. Some of the most recent contributions to the FE analysis of piezoelectric shells that are based on exact geometry solid-shell element with the first-order seven-parameter equivalent single-layer (ESL) theory have been developed by Kulikov et al. [35], and a piezoelectric solid-shell element with a mixed variational formulation and a geometrically nonlinear theory has been developed by Klinkel et al. [36].

A plate FE is presented in this article for the analysis of plate structures with piezo-patches. It is based on Carrera's Unified Formulation (CUF), which has been developed by Carrera for multilayered structures [37]. Many works have been devoted to the extension of CUF to electromechanical problems, see [38–41]. Among others, Carrera [42] extends principle of virtual displacement (PVD) and RMVT variational statements to piezo-laminated plates, see also [43–46]. The plate geometry is considered and the MITC method [47–52] is used to contrast the shear locking. The governing equations for the free-vibration analysis of plate structures are derived from the PVD, in order to apply the FE method. An isotropic plate with piezoelectric patches is analyzed, and the results, obtained with the different models contained in CUF, are compared with the higher-order type solution given in the literature by Yasin et al. [53].

2. Unified Formulation

The main feature of the Unified Formulation by Carrera [42] [54,55] is the unified manner in which the displacement variables are handled. According to CUF, the displacement field and the potential field are written by means of approximating functions in the thickness direction as follows:

$$\boldsymbol{u}^k(x,y,z) = F_\tau(z)\boldsymbol{u}^k_\tau(x,y)\ , \quad \delta\boldsymbol{u}^k(x,y,z) = F_s(z)\delta\boldsymbol{u}^k_s(x,y)\ , \quad \tau,s = 0,1,\ldots,N\,, \tag{1}$$

$$\Phi^k(x,y,z) = F_\tau(z)\,\Phi^k_\tau(x,y)\ , \quad \delta\,\Phi^k(x,y,z) = F_s(z)\delta\,\Phi^k_s(x,y)\ , \quad \tau,s = 0,1,\ldots,N\,, \tag{2}$$

where (x, y, z) is a Cartesian coordinate reference system, defined in the next section, and the displacement $\boldsymbol{u} = \{u, v, w\}$ and the potential Φ are referred to such system. δ indicates the virtual variation and $k = 1, \ldots, n_l$ identifies the layer where n_l is the total number of layers. In this work, the layer number n_l assumes two values: $n_l = 1$ for the plate and $n_l = 3$ for the plate area in with both sensors and/or actuators are present. F_τ and F_s are the so-called thickness functions depending only on z. $\boldsymbol{u}_s$ and Φ_s are the unknown variables depending on the coordinates x and y. τ and s are sum indexes and N is the order of expansion in the thickness direction assumed for the variables. In the case of ESL models, a Taylor expansion is employed as thickness functions:

$$\boldsymbol{u} = F_0\,\boldsymbol{u}_0 + F_1\,\boldsymbol{u}_1 + \ldots + F_N\,\boldsymbol{u}_N = F_s\,\boldsymbol{u}_s, \qquad s = 0, 1, \ldots, N. \tag{3}$$

$$F_0 = z^0 = 1, \quad F_1 = z^1 = z, \quad \ldots, \quad F_N = z^N. \tag{4}$$

Classical theories, such as the FSDT, can be obtained from an ESL model with $N = 1$, by imposing a constant transverse displacement through the thickness via penalty techniques. The correction of the Poisson's locking is applied to the FSDT model and the ESL model with $N = 1$ according to the procedure explained in the literature [56].

In the case of LW models, the displacement and the potential are defined at the k-layer level:

$$\boldsymbol{u}^k = F_t\,\boldsymbol{u}_t^k + F_b\,\boldsymbol{u}_b^k + F_r\,\boldsymbol{u}_r^k = F_\tau\,\boldsymbol{u}_\tau^k, \qquad \tau = t, b, r\,, \quad r = 2, \ldots, N. \tag{5}$$

$$\Phi^k = F_t\,\Phi_t^k + F_b\,\Phi_b^k + F_r\,\Phi_r^k = F_\tau\,\Phi_\tau^k, \qquad \tau = t, b, r\,, \quad r = 2, \ldots, N. \tag{6}$$

$$F_t = \frac{P_0 + P_1}{2}, \quad F_b = \frac{P_0 - P_1}{2}, \quad F_r = P_r - P_{r-2}. \tag{7}$$

in which $P_j = P_j(\zeta_k)$ is the Legendre polynomial of j-order defined in the ζ_k-domain: $P_0 = 1$, $P_1 = \zeta_k$, $P_2 = (3\zeta_k^2 - 1)/2$, $P_3 = (5\zeta_k^3 - 3\zeta_k)/2$, $P_4 = (35\zeta_k^4 - 30\zeta_k^2 + 3)/8$. The top ($t$) and bottom ($b$) values of the displacements and the potential are used as unknown variables, and one can impose the following compatibility conditions:

$$\boldsymbol{u}_t^k = \boldsymbol{u}_b^{k+1}, \quad \Phi_t^k = \Phi_b^{k+1}, \quad k = 1,\ n_l - 1. \tag{8}$$

The LW models, in respect to the ESLs, allow the zigzag form of the variable distribution in layered structures to be modelled.

3. Plate geometry

In this section, the derivation of a plate FE for the analysis of multilayered structures is presented. The element is based on LW and ESL theories contained in the Unified Formulation. A nine-node plate element is considered. Plates are bi-dimensional structures in which one dimension (in general the thickness in the z-direction) is negligible with respect to the other two in-plane dimensions. In this work, the layer number n_l assumes two values: $n_l = 1$ for the plate, $n_l = 3$ for the plate area in which both sensors and/or actuators are present. Geometry and the reference system are indicated in Figure 1. Geometrical relations can be expressed in matrix form as:

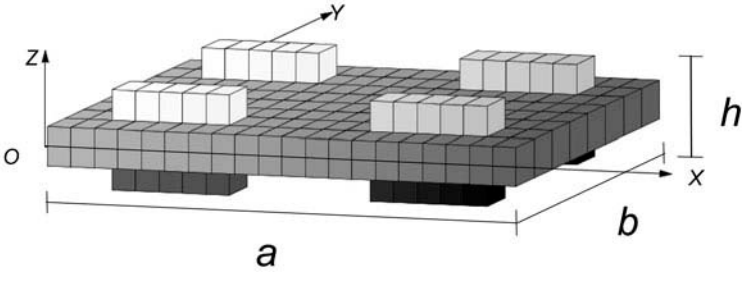

Figure 1. Geometry of the plate.

$$\begin{aligned}\boldsymbol{\sigma}_p &= [\sigma_{xx}, \sigma_{yy}, \gamma_{xy}] = (\boldsymbol{D}_p)\boldsymbol{u}\,,\\ \boldsymbol{\sigma}_n &= [\gamma_{xz}, \gamma_{yz}, \sigma_{zz}] = (\boldsymbol{D}_{np} + \boldsymbol{D}_{nz})\boldsymbol{u}\,,\end{aligned} \tag{9}$$

where the differential operators are defined as follows:

$$\boldsymbol{D}_p = \begin{bmatrix}\partial_x & 0 & 0\\ 0 & \partial_y & 0\\ \partial_y & \partial_x & 0\end{bmatrix} \boldsymbol{D}_{np} = \begin{bmatrix}0 & 0 & \partial_x\\ 0 & 0 & \partial_y\\ 0 & 0 & 0\end{bmatrix} \boldsymbol{D}_{nz} = \begin{bmatrix}\partial_z & 0 & 0\\ 0 & \partial_z & 0\\ 0 & 0 & \partial_z\end{bmatrix} \tag{10}$$

The geometrical relations between electric field **E** and potential Φ are defined as follows:

$$\begin{aligned}\mathrm{E}_p &= [\mathrm{E}_x, \mathrm{E}_y]^T = -\boldsymbol{D}_{ep}\,\Phi\,,\\ \mathrm{E}_n &= [\mathrm{E}_z]^T = -\boldsymbol{D}_{en}\,\Phi\,,\end{aligned} \tag{11}$$

where the differential operators are defined as follows:

$$\boldsymbol{D}_{ep} = \begin{bmatrix}\partial_x\\ \partial_y\end{bmatrix}, \boldsymbol{D}_{en} = [\partial_z].$$

4. Finite-element approximation and MITC method

According to the FE method, the displacement and the potential components are interpolated on the nodes of the element by means of the Lagrangian shape functions *Ni*:

$$\delta\boldsymbol{u}_s = N_i\delta\boldsymbol{q}_{us_i} \qquad \boldsymbol{u}_\tau = N_j\boldsymbol{q}_{u\tau_j} \qquad \text{with} \quad i,j = 1,\ldots,9 \tag{12}$$

$$\delta\Phi_s = N_i\delta q_{\Phi s_i} \qquad \Phi_\tau = N_j q_{\Phi\tau_j} \qquad \text{with} \quad i,j = 1,\ldots,9 \tag{13}$$

where $\boldsymbol{q}_{u\tau_j} = (\boldsymbol{q}_{u_\tau}, \boldsymbol{q}_{v_\tau}, \boldsymbol{q}_{w_\tau})$ and $\delta\boldsymbol{q}_{us_i} = (\delta\boldsymbol{q}_{u_s}, \delta\boldsymbol{q}_{v_s}, \delta\boldsymbol{q}_{w_s})$ are the nodal displacements and their virtual variations for the mechanical variables, and $q_{\Phi\tau_j} = (q_{\Phi_\tau})$ and $\delta q_{\Phi s_i} = (\delta q_{\Phi_s})$ are the nodal potential and their virtual variation for the electric variable. Substituting in the geometrical relations (9), one has:

$$\begin{aligned}\boldsymbol{\epsilon}_p &= F_\tau\,(\boldsymbol{D}_p)(N_i)\boldsymbol{q}_{\boldsymbol{\tau}_i}\\ \boldsymbol{\epsilon}_n &= F_\tau\,(\boldsymbol{D}_{n\Omega})(N_i)\boldsymbol{q}_{\boldsymbol{\tau}_i} + F_{\tau_z}\boldsymbol{D}_{nz}(N_i)\boldsymbol{q}_{\boldsymbol{\tau}_i}\end{aligned} \tag{14}$$

Considering the local coordinate system (ξ, η), the MITC plate elements [57,58] are formulated by using, instead of the strain components directly computed from the displacements, an interpolation of these within each element using a specific interpolation strategy for each component. The corresponding interpolation points, called tying points, are shown in Figure 2 for the MITC9 plate element.

The interpolating functions are Lagrangian and are calculated by imposing that the function assumes the value 1 in the corresponding tying point and 0 in the others. These are arranged in the following arrays:

$$\begin{aligned}\boldsymbol{N}_{m1} &= [N_{A1}, N_{B1}, N_{C1}, N_{D1}, N_{E1}, N_{F1}]\\ \boldsymbol{N}_{m2} &= [N_{A2}, N_{B2}, N_{C2}, N_{D2}, N_{E2}, N_{F2}]\\ \boldsymbol{N}_{m3} &= [N_P, N_Q, N_R, N_S]\end{aligned} \tag{15}$$

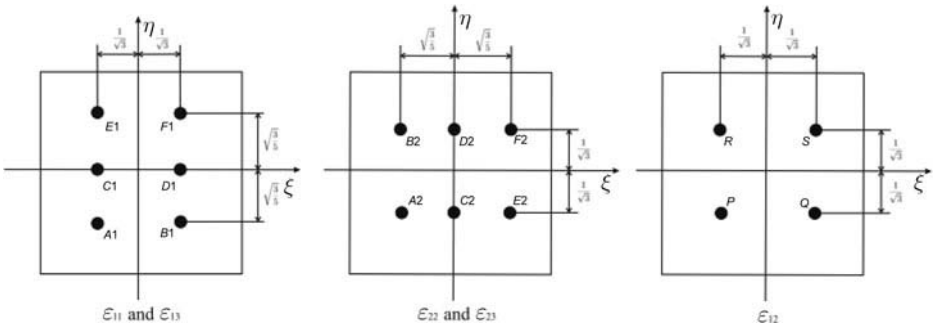

Figure 2. Tying points for the MITC9 shell finite element.

From this point on, the subscripts $m1$, $m2$, and $m3$ indicate quantities calculated in the points ($A1$, $B1$, $C1$, $D1$, $E1$, $F1$), ($A2$, $B2$, $C2$, $D2$, $E2$, $F2$) and (P, Q, R, S), respectively. Therefore, the strain components are interpolated as follows:

$$\begin{aligned}\boldsymbol{\epsilon}_{\mathrm{p}} &= \begin{bmatrix}\epsilon_{\mathrm{xx}}\\ \epsilon_{\mathrm{yy}}\\ \gamma_{\mathrm{xy}}\end{bmatrix} = \begin{bmatrix}\mathbf{N}_{\mathrm{m1}} & 0 & 0\\ 0 & \mathbf{N}_{\mathrm{m2}} & 0\\ 0 & 0 & \mathbf{N}_{\mathrm{m3}}\end{bmatrix}\begin{bmatrix}\epsilon_{\mathrm{xx_{m1}}}\\ \epsilon_{\mathrm{yy_{m2}}}\\ \gamma_{\mathrm{xy_{m3}}}\end{bmatrix}\\ \boldsymbol{\epsilon}_{\mathrm{n}} &= \begin{bmatrix}\gamma_{\mathrm{xz}}\\ \gamma_{\mathrm{yz}}\\ \epsilon_{\mathrm{zz}}\end{bmatrix} = \begin{bmatrix}\mathbf{N}_{\mathrm{m1}} & 0 & 0\\ 0 & \mathbf{N}_{\mathrm{m2}} & 0\\ 0 & 0 & 1\end{bmatrix}\begin{bmatrix}\gamma_{\mathrm{xz_{m1}}}\\ \gamma_{\mathrm{yz_{m2}}}\\ \epsilon_{\mathrm{zz}}\end{bmatrix}\end{aligned} \tag{16}$$

where the strains $\epsilon_{xx_{m1}}$, $\epsilon_{yy_{m2}}$, $\epsilon_{xy_{m3}}$, $\epsilon_{xz_{m1}}$, $\epsilon_{yz_{m2}}$ are expressed by means of Equation (14) and the shape functions N_i are calculated in the tying points.

5. Constitutive equations

The second step toward the governing equations is the definition of the constitutive equations that permit the stresses and the electric displacements to be expressed by means of the strains and the electric fields. The generalized Hooke's law is considered by employing a linear constitutive model for infinitesimal deformations. A linear coupling of the electric fields is employed to complete stress equations and to describe the electric displacement equations. In the numerical section, an isotropic plate with piezo-patches is analyzed, but the constitutive equations have been developed for composite materials as a future extension of this work. These equations are obtained in material coordinates (1, 2, 3) for each layer k and then rotated in the general reference system (x, y, z). Therefore, the stresses $\boldsymbol{\sigma}_p^k = \left\{\sigma_{xx}^k, \sigma_{yy}^k, \gamma_{xy}^k\right\}$ and $\boldsymbol{\sigma}_n^k = \left\{\gamma_{xz}^k, \gamma_{yz}^k, \sigma_{zz}^k\right\}$ and electric displacements $\boldsymbol{D}_p^k = \left\{\mathcal{D}_x^k, \mathcal{D}_y^k\right\}$ and $\boldsymbol{D}_n^k = \left\{\mathcal{D}_z^k\right\}$ after the rotation are:

$$\boldsymbol{\sigma}_{pC}^{k} = \boldsymbol{C}_{pp}^{k}\epsilon_{pG}^{k} + \boldsymbol{C}_{pn}^{k}\epsilon_{nG}^{k} - \boldsymbol{e}_{pp}^{k^T}\mathbf{E}_{pG}^{k} - \boldsymbol{e}_{np}^{k^T}\mathbf{E}_{nG}^{k} \tag{17}$$

$$\boldsymbol{\sigma}_{nC}^{k} = \boldsymbol{C}_{np}^{k}\epsilon_{pG}^{k} + \boldsymbol{C}_{nn}^{k}\epsilon_{nG}^{k} - \boldsymbol{e}_{pn}^{k^T}\mathbf{E}_{pG}^{k} - \boldsymbol{e}_{nn}^{k^T}\mathbf{E}_{nG}^{k} \tag{18}$$

$$\boldsymbol{D}_{pC}^{k} = \boldsymbol{e}_{pp}^{k}\epsilon_{pG}^{k} + \boldsymbol{e}_{pn}^{k}\epsilon_{nG}^{k} + \boldsymbol{\varepsilon}_{pp}^{k}\mathbf{E}_{pG}^{k} + \boldsymbol{\varepsilon}_{pn}^{k}\mathbf{E}_{nG}^{k} \tag{19}$$

$$\boldsymbol{D}_{nC}^{k} = \boldsymbol{e}_{np}^{k}\epsilon_{pG}^{k} + e_{nn}^{k}\epsilon_{nG}^{k} + \boldsymbol{\varepsilon}_{np}^{k}\mathbf{E}_{pG}^{k} + \boldsymbol{\varepsilon}_{nn}^{k}\mathbf{E}_{nG}^{k} \tag{20}$$

where

$$\begin{aligned} \boldsymbol{C}_{pp}^{k} &= \begin{bmatrix} C_{11}^{k} & C_{12}^{k} & C_{16}^{k} \\ C_{12}^{k} & C_{22}^{k} & C_{26}^{k} \\ C_{16}^{k} & C_{26}^{k} & C_{66}^{k} \end{bmatrix} \quad \boldsymbol{C}_{pn}^{k} = \begin{bmatrix} 0 & 0 & C_{13}^{k} \\ 0 & 0 & C_{23}^{k} \\ 0 & 0 & C_{36}^{k} \end{bmatrix} \\ \boldsymbol{C}_{np}^{k} &= \begin{bmatrix} 0 & 0 & 0 \\ 0 & 0 & 0 \\ C_{13}^{k} & C_{23}^{k} & C_{36}^{k} \end{bmatrix} \quad \boldsymbol{C}_{nn}^{k} = \begin{bmatrix} C_{55}^{k} & C_{45}^{k} & 0 \\ C_{45}^{k} & C_{44}^{k} & 0 \\ 0 & 0 & C_{33}^{k} \end{bmatrix} \end{aligned} \tag{21}$$

$$\begin{aligned} \boldsymbol{e}_{pp}^{k} &= \begin{bmatrix} 0 & 0 & 0 \\ 0 & 0 & 0 \end{bmatrix}, \quad \boldsymbol{e}_{pn}^{k} = \begin{bmatrix} e_{15}^{k} & e_{14}^{k} & 0 \\ e_{25}^{k} & e_{24}^{k} & 0 \end{bmatrix}, \\ \boldsymbol{e}_{np}^{k} &= \begin{bmatrix} e_{31}^{k} & e_{32}^{k} & e_{36}^{k} \end{bmatrix}, \quad \boldsymbol{e}_{nn}^{k} = \begin{bmatrix} 0 & 0 & e_{33}^{k} \end{bmatrix}. \end{aligned} \tag{22}$$

$$\boldsymbol{\varepsilon}_{pp}^{k} = \begin{bmatrix} \varepsilon_{11}^{k} & \varepsilon_{12}^{k} \\ \varepsilon_{12}^{k} & \varepsilon_{22}^{k} \end{bmatrix}, \quad \boldsymbol{\varepsilon}_{pn}^{k} = \begin{bmatrix} 0 \\ 0 \end{bmatrix}, \quad \boldsymbol{\varepsilon}_{np}^{k} = \begin{bmatrix} 0 & 0 \end{bmatrix}, \quad \boldsymbol{\varepsilon}_{nn}^{k} = \begin{bmatrix} \boldsymbol{\varepsilon}_{33}^{k} \end{bmatrix}. \tag{23}$$

The material coefficients *Cij* depend on the Young's moduli E_1, E_2, E_3, the shear moduli G_{12}, G_{13}, G_{23} and Poisson moduli ν_{12}, ν_{13}, ν_{23}, ν_{21}, ν_{31}, ν_{32} that characterize the layer material. The piezoelectric material is characterized by the piezoelectric stiffness coefficients *eij* and the permittivity coefficients εij. For the problem analyzed in this work, the piezoelectric stiffness coefficients are calculated from the piezoelectric coefficients *dij* as follows:

$$\mathbf{e}^{k^T} = \mathbf{C}^{k}\,\mathbf{d}^{k^T} \tag{24}$$

where

$$\begin{aligned} \boldsymbol{d}_{pp}^{k} &= \begin{bmatrix} 0 & 0 & 0 \\ 0 & 0 & 0 \end{bmatrix}, \quad \boldsymbol{d}_{pn}^{k} = \begin{bmatrix} d_{15}^{k} & d_{14}^{k} & 0 \\ d_{25}^{k} & d_{24}^{k} & 0 \end{bmatrix}, \\ \boldsymbol{d}_{np}^{k} &= \begin{bmatrix} d_{31}^{k} & d_{32}^{k} & d_{36}^{k} \end{bmatrix}, \quad \boldsymbol{d}_{nn}^{k} = \begin{bmatrix} 0 & 0 & d_{33}^{k} \end{bmatrix}. \end{aligned} \tag{25}$$

6. Governing equations and FE matrices

This section presents the derivation of the governing FE stiffness matrix based on the PVD in the case of multilayered plate structures subjected to electromechanical loads. The PVD for a multilayered piezoelectric structure reads:

$$\int_{V} \left(\delta\boldsymbol{\epsilon}_{pG}{}^{T}\boldsymbol{\sigma}_{pC} + \delta\boldsymbol{\epsilon}_{nG}{}^{T}\boldsymbol{\sigma}_{nC} - \delta\mathbf{E}_{pG}^{T}\boldsymbol{D}_{pC} - \delta\mathbf{E}_{pG}^{T}\boldsymbol{D}_{\mathrm{pC}} \right) dV = \delta L_{\mathrm{e}} - \delta L_{\mathrm{in}} \tag{26}$$

where V is the volume, integration domain of the structure. The first member of the equation represents the variation of the internal work, while the second members are

respectively the external work δL_{e} and the inertial work δL_{in}. In order to refer the integration domains to the midsurface of each layer Ω_k in the plate coordinate system and along the thickness direction A_k, one has to introduce the following integral notation:

$$\int_{\Omega_k}\int_{A_k}\left\{\delta\boldsymbol{\epsilon}_{pG}^{k\ T}\boldsymbol{\sigma}_{pC}^{k}+\delta\boldsymbol{\epsilon}_{nG}^{k\ T}\boldsymbol{\sigma}_{nC}^{k}-\delta\mathbf{E}_{pG}^{k\ T}\boldsymbol{D}_{pC}^{k}-\delta\mathbf{E}_{pG}^{k\ T}\boldsymbol{D}_{pC}^{k}\right\}d\Omega_k dz=\delta L_{\mathrm{e}}-\delta L_{\mathrm{in}} \tag{27}$$

where

$$\delta L_{\mathrm{in}}=\int_{\Omega_k}\int_{A_k}\left\{\rho\,\delta\boldsymbol{u}^T\ddot{\boldsymbol{u}}\right\}d\Omega_k dz \tag{28}$$

$\boldsymbol{u}$ are the general unknown displacements, $\ddot{\boldsymbol{u}}$ are the accelerations, and ρ is the material density. $\delta L_{\mathrm{e}}=0$ in the case of free-vibration analysis.

Substituting the constitutive Equations (17–20), the geometrical relations written via the MITC method (16) and applying the Unified Formulation 1 and the FEM approximation 12, one obtains the following governing equations:

$$\delta\boldsymbol{u}_s^k:\boldsymbol{K}_{uu}^{k\tau s}\boldsymbol{u}_\tau^k+\boldsymbol{K}_{u\Phi}^{k\tau s}\boldsymbol{\Phi}_\tau^k=-\boldsymbol{M}_{uu}^{k\tau s}\ddot{\boldsymbol{u}}_\tau^k \tag{29}$$

$$\delta\boldsymbol{\Phi}_s^k:\boldsymbol{K}_{\Phi u}^{k\tau s}u_\tau^k+\boldsymbol{K}_{\Phi\Phi}^{k\tau s}\boldsymbol{\Phi}_\tau^k=0 \tag{30}$$

In compact form:

$$\delta\boldsymbol{q}_s^k:\boldsymbol{K}^{k\tau s}\boldsymbol{q}_\tau^k=-\boldsymbol{M}^{k\tau s}\ddot{\boldsymbol{q}}_\tau^k \tag{31}$$

where

$$\boldsymbol{K}^{k\tau s}=\begin{bmatrix}\boldsymbol{K}_{uu} & \boldsymbol{K}_{u\Phi}\\ \boldsymbol{K}_{\Phi u} & \boldsymbol{K}_{\Phi\Phi}\end{bmatrix}^{k\tau s},\quad \boldsymbol{M}^{k\tau s}=\begin{bmatrix}\boldsymbol{M}_{uu} & 0\\ 0 & 0\end{bmatrix}^{k\tau s} \tag{32}$$

The undamped dynamic problem can be written as follows:

$$\boldsymbol{M}^{k\tau s}\ddot{\boldsymbol{q}}_\tau^k+\boldsymbol{K}^{k\tau s}\boldsymbol{q}_\tau^k=0 \tag{33}$$

Introducing harmonic solutions, it is possible to compute the natural frequencies ω_n by solving an eigenvalue problem:

$$(\boldsymbol{K}^{k\tau s}-\omega_n^2\boldsymbol{M}^{k\tau s})\boldsymbol{q}_\tau^k=0 \tag{34}$$

where q_τ^k are the eigenvectors. The mechanical part $\boldsymbol{K}_{uu}^{k\tau sij}$is a 3×3 matrix, the coupling matrices $\boldsymbol{K}_{u\phi}^{k\tau sij}$ and $\boldsymbol{K}_{\phi u}^{k\tau sij}$have dimensions 3×1 and 1×3, respectively, and the electrical part $\boldsymbol{K}_{\phi\phi}^{k\tau sij}$is a 1×1 matrix. This is the basic element from which the stiffness matrix of the whole structure is computed. The mechanical part of the mass matrix $\boldsymbol{M}_{uu}^{k\tau sij}$ is a 3 × 3 matrix, the other parts of the global mass matrix are imposed to zero. The global matrix

$\boldsymbol{K}^{k\tau sij}$ and $\boldsymbol{M}^{k\tau sij}$ are called fundamental nucleus, and their explicit expression is given in Appendix 1. For the expansion of the fundamental nucleus on the indexes τ and s and the assembling procedure at multilayer level, the reader can refer to [42]. $q_\tau = (q_{u_\tau}, q_{v_\tau}, q_{w_\tau}, q_{\Phi_\tau})$ is the vector of the nodal mechanical displacements and the nodal electric potential.

7. Numerical results and discussion

In this work, a simple displacement formulation is employed for the analysis of plate structures with piezoelectric patches. The refined theories contained in CUF, coupled with the MITC method, permit a high degree of accuracy to be reached by increasing the order of expansion of displacements in the thickness direction and the number of used elements. In the electromechanical problems, it is necessary to impose the values of the electric potential variable at the top and bottom surfaces of the plate. To obtain this, LW models with Legendre polynomials are particularly suitable. The efficiency of LW models is tested with the FE scheme, and the numerical results are compared with those presented in the literature. In this direction, two kinds of reference problems are considered: an aluminum rectangular plate with eight piezoelectric patches symmetrically placed (four on the top and four on the bottom surfaces) in short- and open-circuit configurations. In this article, some acronyms are used in tables and figures to indicate models employed. The first part indicates the multilayer approach, LW or ESL. The number N indicates the order of expansion used in the thickness direction.

7.1. *Cantilevered plate with piezo-patches*

The structure analyzed by Yasin et al. [53] (see Figure 3) is a cantilevered aluminum plate with eight piezoelectric patches, four on the top surface and symmetrically four on the bottom ones. The plate is clamped on one short edge and free on the other three sides. The physical and geometrical properties of the plate are given in Table 1. A convergence study is

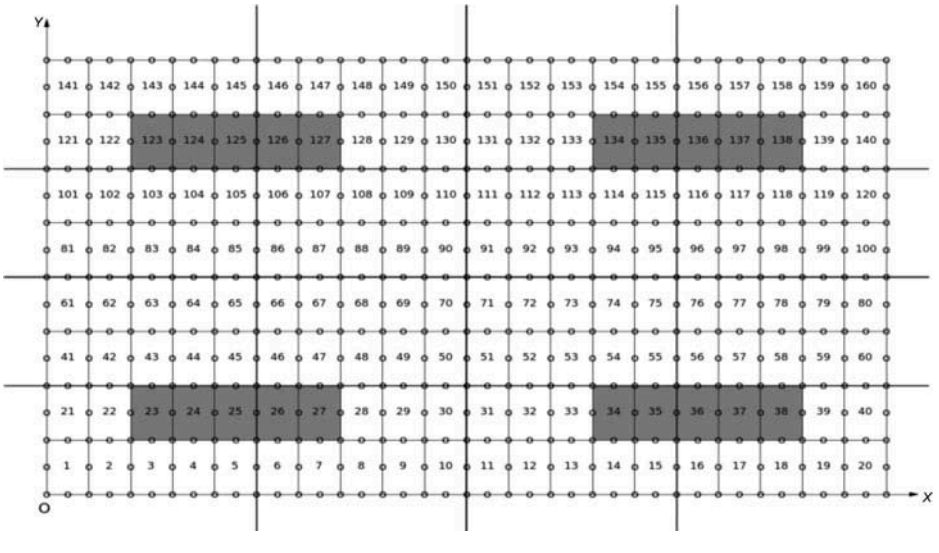

Figure 3. Mesh adopted for the isotropic plate with piezo-patches.

Table 1. Physical and geometrical data of the cantilevered plate with piezoelectric patches.

Material	PZT	Aluminum
a [m]	0.075	0.3
b [m]	0.025	0.2
h [m]	0.63×10^{-3}	0.8×10^{-3}
Density [K g/m^3]	7600.0	2700.0
E_{11} [N/m^2]	63.0×10^{9}	70.0×10^{9}
E_{22} [N/m^2]	63.0×10^{9}	70.0×10^{9}
E_{33} [N/m^2]	63.0×10^{9}	70.0×10^{9}
ν_{12} [−]	0.28	0.32
ν_{13} [−]	0.28	0.32
ν_{23} [−]	0.28	0.32
G_{12} [N/m^2]	24.8×10^{9}	26.515×10^{9}
G_{13} [N/m^2]	24.8×10^{9}	26.515×10^{9}
G_{23} [N/m^2]	24.8×10^{9}	26.515×10^{9}
d_{15} [m/V]	670.0×10^{-12}	0
d_{24} [m/V]	670.0×10^{-12}	0
d_{31} [m/V]	-220.0×10^{-12}	0
d_{32} [m/V]	-220.0×10^{-12}	0
d_{33} [m/V]	374.0×10^{-12}	0
ε_{11} [F/m]	15.3×10^{-9}	30.975×10^{-12}
ε_{22} [F/m]	15.3×10^{-9}	26.55×10^{-12}
ε_{33} [F/m]	15.0×10^{-9}	26.55×10^{-12}

Table 2. Convergence study.

Mesh	10 × 4	20 × 8
1	7.6526	7.6074
2	25.967	25.351
3	46.379	45.790
4	92.789	90.454
5	126.01	123.76
6	153.40	149.00
7	189.47	184.88
8	249.12	235.48
9	316.52	327.03
10	347.66	332.31

Frequencies of a cantilevered plate with piezo-patches. Open-circuit configuration. LW4 model.

presented in Table 2 for the open-circuit configuration, and the LW4 model is employed. Two meshes are considered: 10 × 4 and 20 × 8 elements (this last is represented in Figure 3). Since the results show small differences, the mesh 20 × 8 can be taken as convergence solution, and it will be adopted for the following analysis. First of all, a comparison between the MITC method and the selective reduced integration technique is presented in Table 3 for both short- and open-circuit configurations, and the LW4 model is employed. The table shows that the present MITC9 element is as efficient in contrasting the shear locking phenomenon as classical reduced integration techniques. Moreover, in the work [49], it was demonstrated that the MITC method permits the spurious modes to be reduced/removed.

Table 3. Frequencies of a cantilevered plate with piezo-patches.

	Short circuit		Open circuit	
Mode	MITC	Selective	MITC	Selective
1	7.6059	7.5897	7.6074	7.5914
2	25.346	25.306	25.351	25.313
3	45.787	45.732	45.790	45.737
4	90.446	90.250	90.454	90.274
5	123.76	123.62	123.76	123.64
6	148.93	148.23	149.00	148.28
7	184.69	184.02	184.88	184.09
8	235.50	234.94	235.48	235.01
9	328.22	327.38	327.03	327.46
10	332.49	329.79	332.31	329.96

Comparison between MITC method and selective reduced integration technique. Short- and open-circuit configurations. LW4 model.

7.1.1. Short-circuit mode

For the first case, the piezoelectric patches are short circuited, thereby rendering ineffective the piezoelectric coupling effect that enhances the stiffness of otherwise passive structure. This case includes only the pure structural stiffness of the PZT patches and the modal analysis, made by Yasin et al. [53], involves the solution of the simplified following eigenvalue problem:

$$(\boldsymbol{K}_{uu} - \omega_n^2 \boldsymbol{M})\,\boldsymbol{q}_n = 0$$

In this work, two methods are used for short-circuit mode: the free-vibration analysis using the mechanical stiffness only, as Yasin et al. [53], and the free-vibration analysis with the complete stiffness matrix applying the penalty technique for the electrical degrees of freedom of the top and bottom surfaces of piezoelectric patches. In general, the results, given in terms of natural frequencies, approach the exact solution by increasing the order of expansion N, see Table 4. One can note that the element does not suffer the locking phenomenon for the examined thin plate (a/h = 300). The mechanical solution, obtained by using the higher-order LW models, matches the reference solution. The small differences between them can be explained with the different description of the displacement field that in this work is more refined than the reference solution case. The first four modes are shown in Figures 4–7. The solution with the penalty technique applied to the electrical DOFs shows few differences with the mechanical results, see Table 5. This fact is due to the higher-order modeling of the electric potential along the thickness of the patches.

7.1.2. Open-circuit mode

For the second case, the piezoelectric patches are acting as sensors, so in open-circuit mode no electric potential is imposed. A static condensation of the electrical DOFs is made by Yasin et al. [53]:

Table 4. Frequencies of a cantilevered plate with piezo-patches.

Mode	Ref [53]	LW4	LW3	LW2	LW1
1	7.5236	7.5639	7.5640	7.5661	8.2918
2	25.195	25.312	25.324	25.356	26.324
3	45.542	45.718	45.723	45.736	50.113
4	90.215	90.236	90.277	90.386	96.301
5	123.03	123.66	123.69	123.76	133.99
6	147.62	147.08	147.09	147.18	161.14
7	183.16	182.65	182.69	182.85	194.84
8	234.05	235.40	235.51	235.76	254.69
9	326.93	325.14	325.15	325.27	347.75
10	328.04	326.98	327.13	327.52	364.35
Mode	ESL4	ESL3	ESL2	ESL1	FSDT
1	7.7235	7.7318	7.7413	7.6713	7.6882
2	25.654	25.689	25.814	25.737	25.781
3	46.004	46.035	46.072	45.830	45.855
4	91.347	91.459	91.864	91.545	91.667
5	124.78	124.87	125.05	124.75	124.87
6	152.86	153.06	153.45	152.02	152.63
7	188.45	188.61	189.26	187.96	188.51
8	240.23	240.33	241.04	239.63	240.24
9	329.53	329.71	331.25	329.07	329.19
10	343.19	346.92	347.63	342.85	345.16

Pure mechanical case.

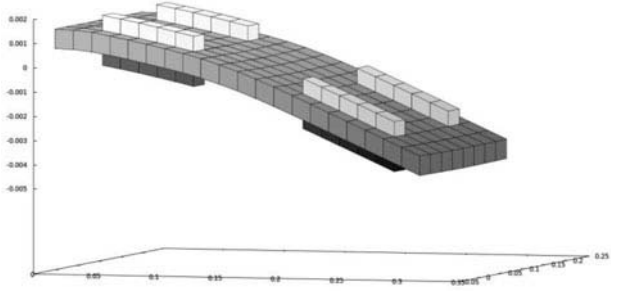

Figure 4. Natural frequency 7.5639 Hz. Mode 1.

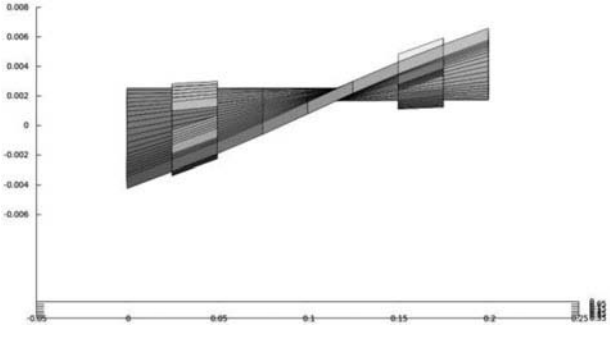

Figure 5. Natural frequency 25.312 Hz. Mode 2.

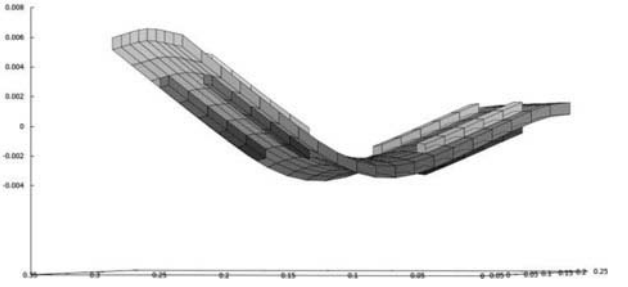

Figure 6. Natural frequency 45.718 Hz. Mode 3.

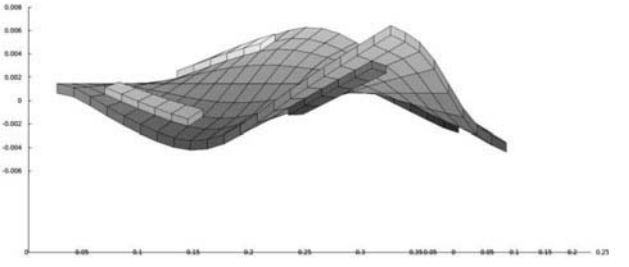

Figure 7. Natural frequency 90.236 Hz. Mode 4.

Table 5. Frequencies of a cantilevered plate with piezo-patches.

Mode	Ref [53]	LW4	LW3	LW2	LW1
1	7.5236	7.6059	7.6061	7.6083	8.3386
2	25.195	25.346	25.359	25.393	26.363
3	45.542	45.787	45.792	45.805	50.190
4	90.215	90.446	90.490	90.607	96.513
5	123.03	123.76	123.79	123.86	134.22
6	147.62	148.93	148.94	149.04	162.99
7	183.16	184.69	184.73	184.91	196.96
8	234.05	235.50	235.62	235.88	254.79
9	326.93	328.22	328.37	328.78	355.13
10	328.04	332.49	332.50	332.64	365.61

Short-circuit case.

$$\left(\left\{\boldsymbol{K}_{uu}-\boldsymbol{K}_{u\Phi}\boldsymbol{K}_{\Phi\Phi}^{-1}\boldsymbol{K}_{\Phi u}^{T}\right\}-\omega_n^2\boldsymbol{M}\right)\boldsymbol{q}_n=0$$

For the open-circuit mode, in this work, free-vibration analysis with complete stiffness matrix is done, see Table 6. In general, the results approach the exact solution by increasing the order of expansion N. One can note that the element does not suffer the locking phenomenon for the examined thin plate (a/h = 300). The higher-order LW models are in good agreement with the reference solution. As in the previous case, there are few differences due to different expansion of the displacement field that in this work is higher-order in respect to the reference solution.

Table 6. Frequencies of a cantilevered plate with piezo-patches.

Mode	Ref [53]	LW4	LW3	LW2	LW1
1	7.5639	7.6074	7.6076	7.6098	8.3402
2	25.221	25.351	25.362	25.396	26.368
3	45.591	45.790	45.795	45.808	50.194
4	90.371	90.454	90.500	90.617	96.526
5	123.10	123.76	123.80	123.87	134.24
6	149.56	149.00	148.98	149.08	163.03
7	185.11	184.88	184.77	184.96	197.01
8	234.05	235.48	235.65	235.91	254.83
9	328.18	327.03	328.40	328.81	355.22
10	335.68	332.31	332.59	332.73	365.65

Open-circuit case.

7.1.3. *Benchmark solutions*

Table 7 shows the first 10 natural frequencies of the same structures, but considering two different geometries: in the first one, the thickness of the aluminum plate and patches is multiplied by 10; in the second case, it is divided by 10. Both short- and open-circuit configurations are studied and the models LW1 and LW4 are employed for the analysis. Since no reference results are provided in the literature for these cases, the solutions presented can be used as benchmark solutions for future comparisons.

8. Conclusion

This article has presented the free-vibration analysis of an isotropic plate with piezo-patches by means of a plate FE based on the CUF [54,55]. The results have been provided in terms of free-vibration natural frequencies for very thin plates, and the performances of the various models, equivalent-single-layer and LW theories contained in CUF, have been tested. The conclusions that can be drawn are the following:

Table 7. Frequencies of a cantilevered plate with piezo-patches.

	*h*new = *h* * 10			*h*new = *h*/10				
	Short circuit	Open circuit		Short circuit		Open circuit		
Mode	LW4	LW1	LW4	LW1	LW4	LW1	LW4	LW1
1	74.139	81.481	74.157	81.521	0.7766	0.8454	0.7711	0.8425
2	238.45	247.81	238.84	248.44	2.5428	2.6442	2.5381	2.6425
3	447.52	490.01	447.59	490.18	4.5842	5.0236	4.5837	5.0252
4	853.34	908.09	854.49	910.04	9.0567	9.6632	9.0410	9.6725
5	1176.4	1210.9	1177.1	1211.3	12.388	13.435	12.296	13.431
6	1207.0	1277.2	1207.2	1278.2	14.927	16.324	15.329	16.322
7	1411.9	1551.3	1412.8	1552.8	18.509	19.729	19.027	19.791
8	1733.1	1851.8	1734.6	1854.4	23.593	25.520	23.517	25.601
9	2147.1	2328.3	2151.0	2334.1	32.863	35.573	30.072	34.862
10	3023.0	3322.6	3024.8	3327.9	33.325	36.602	31.904	36.237

Different aspect ratios.

(1) the plate element is locking free when the plate is very thin;
(2) the exact solution is achieved by increasing the order of expansion of the variables in the thickness;
(3) the use of LW models gives more accurate results, if the free-vibration behavior of the structure needs to be accurately described;
(4) the analysis of short-circuit mode shows that the higher-order description of the electric potential gives some differences in the frequency results compared to those obtained with pure mechanical analysis;
(5) Future works could be devoted to extending this plate element to shell structure with single or double curvature.

Disclosure statement

No potential conflict of interest was reported by the authors.

References

[1] A.K. Noor and W.S. Burton, *Assessment of computational models for multilayered shells*, Appl. Mech. Rev. 43(4) (1990), pp. 67–97.
[2] E. Crawley and J. De Luis, *Use of piezoelectric actuators as elements of intelligent structures*, AIAA J. 25 (1987), pp. 1373–1385. doi:10.2514/3.9792.
[3] T. Bailey and J. Hubbard, *Distributed piezoelectric polymer active vibration control of a cantilever beam*, AIAA J. 8 (1985), pp. 605–611.
[4] D. Robbins and J. Reddy, Analysis of piezoelectrically actuated beams using a layer-wise displacement theory, Comput. Struct. 41 (1991a), pp. 265–279. doi:10.1016/0045-7949(91)90430-T.
[5] E. Carrera, *Historical review of zig-zag theories for multilayered plates and shells*, Appl. Mech. Rev. 56(3) (2003), pp. 287–308.
[6] J.N. Reddy, *Mechanics of Laminated Composite Plates and Shells: Theory and Analysis*, CRC Press, Boca Raton, 2004.
[7] E. Carrera, *CZ requirements—Models for the two dimensional analysis of multilayered structures*, Composite Struct. 37 (1997), pp. 373–383. doi:10.1016/S0263-8223(98)80005-6.
[8] W.T. Koiter, *A consistent first approximation in the general theory of thin elastic shells*, in *The Theory of Thin Elastic Shells*, W.T. Koiter, ed., IUTAM, Delft, North-Holland, 1959, pp. 12–33.
[9] R.D. Mindlin, *Forced thickness-shear and flexural vibrations of piezoelectric crystal plates*, J. Appl. Phys. 23 (1952), pp. 83–88.
[10] E.P. EerNisse, *Variational method for electroelastic vibration analysis*, IEEE Trans. Sonics Ultra- Sonics 14(4) (1967), pp. 153–159. doi:10.1109/T-SU.1967.29431.
[11] H.F. Tiersten and R.D. Mindlin, *Forced vibrations of piezoelectric crystal plates*, Quart. Appl. Math. 20(2) (1962), pp. 107–119.
[12] H.F. Tiersten, *Linear Piezoelectric Plate Vibrations*, Plenum, New York, 1969.
[13] D.A. Saravanos and P.R. Heyliger, *Mechanics and computational models for laminated piezoelectric beams, plates and shells*, Appl. Mech. Rev. 52(10) (1999), pp. 305–319.
[14] S. Kapuria, *A coupled zig-zag third-order theory for piezoelectric hybrid cross-ply plates*, J. Appl. Mech. 71 (2004), pp. 604–614.
[15] C. Ossadzow-David and M. Touratier, *A multilayered piezoelectric shell theory*, Compos. Sci. Technol. 64 (2004), pp. 2121–2137. doi:10.1016/j.compscitech.2004.03.005.
[16] P. Heyliger, K.C. Pei, and D.A. Saravanos, Layerwise mechanics and finite element model for laminated piezoelectric shells, AIAA J. 34(11) (1996), pp. 2353–2360. doi:10.2514/3.13401.
[17] D. Ballhause, M. D'Ottavio, B. Kröplin, and E. Carrera, *A unified formulation to assess multilayered theories for piezoelectric plates*, Comput. Struct. 83(15–16) (2005), pp. 1217–1235. doi:10.1016/j.compstruc.2004.09.015.

[18] M. D'Ottavio, D. Ballhause, B. Kroeplin, and E. Carrera, *Closed-form solutions for the free-vibration problem of multilayered piezoelectric shells*, Comput. Struct. 84 (2006), pp. 1506–1518. doi:10.1016/j.compstruc.2006.01.030.
[19] A. Benjeddou, J. Deu, and S. Letombe, *Free vibrations of simply-supported piezoelectric adaptive plates: An exact sandwich formulation*, Thin-Walled Struct. 40 (2002), pp. 573–593. doi:10.1016/S0263-8231(02)00013-7.
[20] N.N. Rogacheva, *The Theory of Piezoelectric Shells and Plates*, CRC Press, Boca Raton, 1994
[21] X. Zhou, A. Chattopadhyay, and H. Gu, Dynamic responses of smart composites using a coupled thermo-piezoelectric-mechanical model, AIAA J. 38 (2000), pp. 1939–1948. doi:10.2514/2.848.
[22] A.L. Araújo, C.M.M. Soares, C.A.M. Soares, and J. Herskovits, *Characterisation by inverse techniques of elastic, viscoelastic and piezoelectric properties of anisotropic sandwich adaptive structures*, Appl. Composite Mater. 17(5) (2010), pp. 543–556. doi:10.1007/s10443-010-9142-2.
[23] A.L. Araujo, C.M.M. Soares, and C.A.M. Soares, *Finite element model for hybrid active-passive damping analysis of anisotropic laminated sandwich structures*, J. Sandwich Struct. Mater. 12 (2010), pp. 397–419. doi:10.1177/1099636209104534.
[24] S.V. Gopinathan, V.V. Varadan, and V.K. Varadan, *A review and critique of theories for piezoelectric laminates*, Smart Mater. Struct. 9 (2000), pp. 24–48. doi:10.1088/0964-1726/9/1/304.
[25] A. Benjeddou, *Advances in piezoelectric finite element modeling of adaptive structural elements: A survey*, Comput. Struct. 76 (2000), pp. 347–363. doi:10.1016/S0045-7949(99)00151-0.
[26] R. Lammering and S. Mesecke-Rischmann, *Multi-field variational formulations and related finite elements for piezoelectric shells*, Smart Mater. Struct. 12(6) (2003), pp. 904–913. doi:10.1088/0964-1726/12/6/007.
[27] A. Benjeddou and O. Andrianarison, *Extension of Reissners mixed variational theorem to piezoelectric multilayered composites*, in *Proceedings of the Sixth Hellenic-European Conference on Computer Mathematics and Its Applications*, E.A. Lipitakis, ed., LEA, Athens, Hellas, 2003, pp. 116–124.
[28] A.H. Sheikh, P. Topdar, and S. Halder, An appropriate FE model for through-thickness variation of displacement and potential in thin/moderately thick smart laminates, Composite Struct. 51 (2001), pp. 401–409. doi:10.1016/S0263-8223(00)00156-2.
[29] F. Auricchio, P. Bisegna, and C. Lovadina, *Finite element approximation of piezoelectric plates*, Int. J. Numer. Methods Eng. 50 (2001), pp. 1469–1499. doi:10.1002/(ISSN)1097-0207.
[30] R.P. Thornburgh and A. Chattopadhyay, *Simultaneous modeling of mechanical and electrical response of smart composite structures*, AIAA J. 40(8) (2002), pp. 1603–1610. doi:10.2514/2.1830.
[31] X. Shu, *Free-vibration of laminated piezoelectric composite plates based on an accurate theory*, Composite Struct. 67 (2005), pp. 375–382. doi:10.1016/j.compstruct.2004.01.022.
[32] J. Oh and M. Cho, *A finite element based on cubic zig-zag plate theory for the prediction of thermoelectric-mechanical behaviors*, Int. J. Solids Struct. 41(5–6) (2004), pp. 1357–1375. doi:10.1016/j.ijsolstr.2003.10.019.
[33] M. Kogl and M.L. Bucalem, *Analysis of smart laminates using piezoelectric MITC plate and shell elements*, Comput. Struct. 83 (2005), pp. 1153–1163. doi:10.1016/j.compstruc.2004.08.024.
[34] M. Kogl and M.L. Bucalem, *A family of piezoelectric MITC plate elements*, Comput. Struct. 83 (2005), pp. 1277–1297. doi:10.1016/j.compstruc.2004.04.025.
[35] G.M. Kulikov and S.V. Plotnikova, *Exact geometry piezoelectric solid-shell element based on the 7-parameter model*, Mech. Adv. Mater. Struct. 18 (2011), pp. 133–146. doi:10.1080/15376494.2010.496067.
[36] S. Klinkel and W. Wagner, *A piezoelectric solid shell element based on a mixed variational formulation for geometrically linear and nonlinear applications*, Comput. Struct. 86 (2008), pp. 38–46. doi:10.1016/j.compstruc.2007.05.032.
[37] E. Carrera, *A class of two-dimensional theories for anisotropic multilayered plates analysis*, Accademia Delle Scienze Di Torino, Memorie Sci. Fisiche, 1995-1996 19-20 (1995), pp. 1–39.

[38] A. Robaldo, E. Carrera, and A. Benjeddou, *A unified formulation for finite element analysis of piezo- electric adaptive plates*, Comput. Struct. 84 (2006), pp. 1494–1505. doi:10.1016/j.compstruc.2006.01.029.
[39] E. Carrera, M. Boscolo, and A. Robaldo, *Hierarchic multilayered plate elements for coupled multifield problems of piezoelectric adaptive structures: Formulation and numerical assessment*, Arch. Comput. Methods Eng. 14 (2007), pp. 383–430. doi:10.1007/s11831-007-9012-8.
[40] E. Carrera and A. Robaldo, *Hierarchic finite elements based on a unified formulation for the static analysis of shear actuated multilayered piezoelectric plates*, Multidiscipline Model. Mater. Struct. 6(1) (2010), pp. 45–77. doi:10.1108/15736101011055266.
[41] M. Cinefra, E. Carrera, and S. Valvano, *Variable kinematic shell elements for the analysis of electro-mechanical problems*, SMART 2013 – Modelling and Analysis of Smart Structures, Mech. Adv. Mater. Struct. 22 (2015), pp. 77–106. doi:10.1080/15376494.2014.908042.
[42] E. Carrera, *Theories and finite elements for multilayered plates and shells: A unified compact formulation with numerical assessment and benchmarking*, Arch. Comput. Methods Eng. 10(3) (2003), pp. 215–296. doi:10.1007/BF02736224.
[43] E. Carrera and M. Boscolo, *Classical and mixed finite elements for static and dynamic analysis of piezoelectric plates*, Int. J. Numer. Methods Eng. 70 (2007), pp. 1135–1181. doi:10.1002/(ISSN)1097-0207.
[44] E. Carrera, S. Brischetto, and M. Cinefra, *Variable kinematics and advanced variational statements for free vibrations analysis of piezoelectric plates and shells*, Comput. Model. Eng. Sci. 65(3) (2010), pp. 259–341.
[45] E. Carrera and P. Nali, *Classical and mixed finite plate elements for the analysis of multifield problems and smart layered structures*, Acta Mech. Sinica 23 (2010), pp. 115–121.
[46] E. Carrera and P. Nali, *Multilayered plate elements for the analysis of multifield problems*, Finite Elem. Anal. Des. 46 (2010), pp. 732–742. doi:10.1016/j.finel.2010.04.001.
[47] K.-J. Bathe, P.-S. Lee, and J.-F. Hiller, *Towards improving the MITC9 shell element*, Comput. Struct. 81 (2003), pp. 477–489. doi:10.1016/S0045-7949(02)00483-2.
[48] P. Panasz and K. Wisniewski, *Nine-node shell elements with 6 dofs/node based on two-level approximations. Part I theory and linear tests*, Finite Elem. Anal. Des. 44 (2008), pp. 784–796. doi:10.1016/j.finel.2008.05.002.
[49] E. Carrera, M. Cinefra, and P. Nali, *MITC technique extended to variable kinematic multilayered plate elements*, Composite Struct. 92 (2010), pp. 1888–1895. doi:10.1016/j.compstruct.2010.01.009.
[50] M. Cinefra, C. Chinosi, and L. Della Croce, *MITC9 shell elements based on refined theories for the analysis of isotropic cylindrical structures*, Mech. Adv. Mater. Struct. 20 (2013), pp. 91–100. doi:10.1080/15376494.2011.581417.
[51] M. Cinefra and E. Carrera, *Shell finite elements with different through-the-thickness kinematics for the linear analysis of cylindrical multilayered structures*, Int. J. Numer. Methods Eng. 93 (2013), pp. 160–182. doi:10.1002/nme.4377.
[52] M. Cinefra and S. Valvano, *A variable kinematic doubly-curved MITC9 shell element for the analysis of laminated composites*, Mech. Adv. Mater. Struct. (In Press). ISSN 1537-6494.
[53] M.Y. Yasin, N. Ahmad, and M.N. Alam, *Finite element analysis of actively controlled smart plate with patched actuators and sensors*, Latin American J. of Solids & Struct. 7 (2010), pp. 227–247. doi:10.1590/S1679-78252010000300001.
[54] E. Carrera, *Multilayered shell theories accounting for layerwise mixed description, Part 1: Governing equations*, AIAA J. 37(9) (1999), pp. 1107–1116. doi:10.2514/2.821.
[55] E. Carrera, Multilayered shell theories accounting for layerwise mixed description, Part 2: Numerical evaluations, AIAA J. 37(9) (1999), pp. 1117–1124. doi:10.2514/2.822.
[56] E. Carrera and S. Brischetto, *Analysis of thickness locking in classical, refined and mixed multilayered plate theories*, Composite Struct. 82 (2008), pp. 549–562. doi:10.1016/j.compstruct.2007.02.002.
[57] K.-J. Bathe and E. Dvorkin, *A formulation of general shell elements – the use of mixed interpolation of tensorial components*, Int. J. Numer. Methods Eng. 22 (1986), pp. 697–722. doi:10.1002/(ISSN)1097-0207.
[58] M.L. Bucalem and K.-J. Bathe, *Higher-order MITC general shell elements*, Int. J. Numer. Methods Eng. 36 (1993), pp. 3729–3754. doi:10.1002/(ISSN)1097-0207.

Appendix 1

Explicit form of stiffness fundamental nucleus

In order to write the fundamental nucleus $\boldsymbol{K}$ $k\tau sij$ in compact form, the following integrals in the domain Ω_k are defined:

$$\left(W^k_{m1\,n1};\ W^k_{m1\,n2};\ W^k_{m2\,n1};\ W^k_{m2\,n2}\right) = \int_{\Omega_k} \left(N_{m1}N_{n1};\ N_{m1}N_{n2};\ N_{m2}N_{n1};\ N_{m2}N_{n2}\right)\, dx\,dy$$

$$\left(W^k_{m1\,n3};\ W^k_{m3\,n1};\ W^k_{m3\,n3};\ W^k_{m2\,n3};\ W^k_{m3\,n2}\right) = \int_{\Omega_k} \left(N_{m1}N_{n3};\ N_{m3}N_{n1};\ N_{m3}N_{n3};\ N_{m2}N_{n3};\ N_{m3}N_{n2}\right) dx\,dy$$

$$\left(W^k_{m1\,j};\ W^k_{m2\,j};\ W^k_{m3\,j}\right) = \int_{\Omega_k} \left(N_{m1}N_j;\ N_{m2}N_j;\ N_{m3}N_j\right)\, dx\,dy$$

$$\left(W^k_{in1};\ W^k_{in2};\ W^k_{in3};\ W^k_{ij}\right) = \int_{\Omega_k} \left(N_iN_{n1};\ N_iN_{n2};\ N_iN_{n3};\ N_iN_j\right)\, dx\,dy$$

$$\left(W^k_{m1\,j_{,x}};\ W^k_{m1\,j_{,y}};\ W^k_{m2\,j_{,x}};\ W^k_{m2\,j_{,y}}\right) = \int_{\Omega_k} \left(N_{m1}\frac{\partial N_j}{\partial x};\ N_{m1}\frac{\partial N_j}{\partial y};\ N_{m2}\frac{\partial N_j}{\partial x};\ N_{m2}\frac{\partial N_j}{\partial y}\right)\, dx\,dy$$

$$\left(W^k_{i_{,x}\,n1};\ W^k_{i_{,y}\,n1};\ W^k_{i_{,x}\,n2};\ W^k_{i_{,y}\,n2}\right) = \int_{\Omega_k} \left(\frac{\partial N_i}{\partial x}N_{n1};\ \frac{\partial N_i}{\partial y}N_{n1};\ \frac{\partial N_i}{\partial x}N_{n2};\ \frac{\partial N_i}{\partial y}N_{n2}\right)\, dx\,dy$$

Moreover, the integrals on the domain A_k, in the thickness direction, are written as:

$$\left(J^{k\tau s}; J^{k\tau_z s}; J^{k\tau s_z}; J^{k\tau_z s_z}\right) = \int_{A_k} \left(F_\tau F_s;\ \frac{\partial F_\tau}{\partial z}F_s;\ F_\tau\frac{\partial F_s}{\partial z};\ \frac{\partial F_\tau}{\partial z}\frac{\partial F_s}{\partial z}\right) dz$$

The stiffness fundamental nucleus $\boldsymbol{K}_{\tau sij}$ is:

$$\boldsymbol{K}^{k\tau sij} = \begin{bmatrix} K_{11} & K_{12} & K_{13} & K_{14} \\ K_{21} & K_{22} & K_{23} & K_{24} \\ K_{31} & K_{32} & K_{33} & K_{34} \\ K_{41} & K_{42} & K_{43} & K_{44} \end{bmatrix}^{k\tau sij}$$

The elements of the nucleus are:

$$\begin{aligned} K^{k\tau s}_{uu_{11}} = {} & C^k_{55}N^{(m1)}_i N^{(n1)}_j W^k_{m1\,n1}J^{k\tau_z s_z} + C^k_{66}N^{(m3)}_{i,y}N^{(n3)}_{j,y}W^k_{m3\,n3}J^{k\tau s} \\ & + C^k_{16}N^{(m1)}_{i,x}N^{(n3)}_{j,y}W^k_{m1\,n3}J^{k\tau s} + C^k_{16}N^{(m3)}_{i,y}N^{(n1)}_{j,x}W^k_{m3\,n1}J^{k\tau s} \\ & + C^k_{11}N^{(m1)}_{i,x}N^{(n1)}_{j,x}W^k_{m1\,n1}J^{k\tau s} \end{aligned}$$

$$K^{k\tau s}_{uu_{12}} = C^k_{45} N^{(m1)}_i N^{(n2)}_j W^k_{m1\,n2} J^{k\tau_z s_z} + C^k_{26} N^{(m3)}_{i,y} N^{(n2)}_{j,y} W^k_{m3\,n2} J^{k\tau s} + C^k_{12} N^{(m1)}_{i,x} N^{(n2)}_{j,y} W^k_{m1\,n2} J^{k\tau s} + C^k_{66} N^{(m3)}_{i,y} N^{(n3)}_{j,x} W^k_{m3\,n3} J^{k\tau s} + C^k_{16} N^{(m1)}_{i,x} N^{(n3)}_{j,x} W^k_{m1\,n3} J^{k\tau s}$$

$$K^{k\tau s}_{uu_{13}} = C^k_{45} N^{(m1)}_i N^{(n2)}_{j,y} W^k_{m1\,n2} J^{k\tau_z s} + C^k_{55} N^{(m1)}_i N^{(n1)}_{j,x} W^k_{m1\,n1} J^{k\tau_z s} + C^k_{36} N^{(m3)}_{i,y} W^k_{m3\,j} J^{k\tau s_z} + C^k_{13} N^{(m1)}_{i,x} W^k_{m1\,j} J^{k\tau s_z}$$

$$K^{k\tau s}_{uu_{21}} = C^k_{45} N^{(m2)}_i N^{(n1)}_j W^k_{m2\,n1} J^{k\tau_z s_z} + C^k_{26} N^{(m2)}_{i,y} N^{(n3)}_{j,y} W^k_{m2\,n3} J^{k\tau s} + C^k_{66} N^{(m3)}_{i,x} N^{(n3)}_{j,y} W^k_{m3\,n3} J^{k\tau s} + C^k_{12} N^{(m2)}_{i,y} N^{(n1)}_{j,x} W^k_{m2\,n1} J^{k\tau s} + C^k_{16} N^{(m3)}_{i,x} N^{(n1)}_{j,x} W^k_{m3\,n1} J^{k\tau s}$$

$$K^{k\tau s}_{uu_{22}} = C^k_{44} N^{(m2)}_i N^{(n2)}_j W^k_{m2\,n2} J^{k\tau_z s_z} + C^k_{22} N^{(m2)}_{i,y} N^{(n2)}_{j,y} W^k_{m2\,n2} J^{k\tau s} + C^k_{26} N^{(m3)}_{i,x} N^{(n2)}_{j,y} W^k_{m3\,n2} J^{k\tau s} + C^k_{26} N^{(m2)}_{i,y} N^{(n3)}_{j,x} W^k_{m2\,n3} J^{k\tau s} + C^k_{66} N^{(m3)}_{i,x} N^{(n3)}_{j,x} W^k_{m3\,n3} J^{k\tau s}$$

$$K^{k\tau s}_{uu_{23}} = C^k_{44} N^{(m2)}_i N^{(n2)}_{j,y} W^k_{m2\,n2} J^{k\tau_z s} + C^k_{45} N^{(m2)}_i N^{(n1)}_{j,x} W^k_{m2\,n1} J^{k\tau_z s} + C^k_{23} N^{(m2)}_{i,y} W^k_{m2\,j} J^{k\tau s_z} + C^k_{36} N^{(m3)}_{i,x} W^k_{m3\,j} J^{k\tau s_z}$$

$$K^{k\tau s}_{uu_{31}} = C^k_{36} N^{(n3)}_{j,y} W^k_{i\,n3} J^{k\tau_z s} + C^k_{13} N^{(n1)}_{j,x} W^k_{i\,n1} J^{k\tau_z s} + C^k_{45} N^{(m2)}_{i,y} N^{(n1)}_j W^k_{m2\,n1} J^{k\tau s_z} + C^k_{55} N^{(m1)}_{i,x} N^{(n1)}_j W^k_{m1\,n1} J^{k\tau s_z}$$

$$K^{k\tau s}_{uu_{32}} = C^k_{23} N^{(n2)}_{j,y} W^k_{i\,n2} J^{k\tau_z s} + C^k_{36} N^{(n3)}_{j,x} W^k_{i\,n3} J^{k\tau_z s} + C^k_{44} N^{(m2)}_{i,y} N^{(n2)}_j W^k_{m2\,n2} J^{k\tau s_z} + C^k_{45} N^{(m1)}_{i,x} N^{(n2)}_j W^k_{m1\,n2} J^{k\tau s_z}$$

$$K^{k\tau s}_{uu_{33}} = C^k_{33} W^k_{ij} J^{k\tau_z s_z} + C^k_{44} N^{(m2)}_{i,y} N^{(n2)}_{j,y} W^k_{m2\,n2} J^{k\tau s} + C^k_{45} N^{(m1)}_{i,x} N^{(n2)}_{j,y} W^k_{m1\,n2} J^{k\tau s} + C^k_{45} N^{(m2)}_{i,y} N^{(n1)}_{j,x} W^k_{m2\,n1} J^{k\tau s} + C^k_{55} N^{(m1)}_{i,x} N^{(n1)}_{j,x} W^k_{m1\,n1} J^{k\tau s}$$

$$K^{k\tau s}_{u\Phi_{14}} = e^k_{25} N^{(m1)}_i W^k_{m1\,j_{,y}} J^{k\tau_z s} + e^k_{15} N^{(m1)}_i W^k_{m1\,j_{,x}} J^{k\tau_z s} + e^k_{36} N^{(m3)}_{i,y} W^k_{m3\,j} J^{k\tau s_z} + e^k_{31} N^{(m1)}_{i,x} W^k_{m1\,j} J^{k\tau s_z}$$

$$K^{k\tau s}_{u\Phi_{24}} = e^k_{24} N^{(m2)}_i W^k_{m2\,j_{,y}} J^{k\tau_z s} + e^k_{14} N^{(m2)}_i W^k_{m2\,j_{,x}} J^{k\tau_z s} + e^k_{32} N^{(m2)}_{i,y} W^k_{m2\,j} J^{k\tau s_z} + e^k_{36} N^{(m3)}_{i,x} W^k_{m3\,j} J^{k\tau s_z}$$

$$K^{k\tau s}_{u\Phi_{34}} = e^k_{33} W^k_{ij} J^{k\tau_z s_z} + e^k_{24} N^{(m2)}_{i,y} W^k_{m2\,j_{,y}} J^{k\tau s} + e^k_{25} N^{(m1)}_{i,x} W^k_{m1\,j_{,y}} J^{k\tau s} + e^k_{14} N^{(m2)}_{i,y} W^k_{m2\,j_{,x}} J^{k\tau s} + e^k_{15} N^{(m1)}_{i,x} W^k_{m1\,j_{,x}} J^{k\tau s}$$

$$K_{\Phi u_{41}{}^{k\tau s}} = e^k_{36} N^{(n3)}_{j,y} W^k_{in3} J^{k\tau_z s} + e^k_{31} N^{(n1)}_{j,x} W^k_{in1} J^{k\tau_z s} + e^k_{25} N^{(n1)}_{j} W^k_{i_y n1} J^{k\tau s_z} + e^k_{15} N^{(n1)}_{j} W^k_{i_x n1} J^{k\tau s_z}$$

$$K^{k\tau s}_{\Phi u_{42}} = e^k_{32} N^{(n2)}_{j,y} W^k_{in2} J^{k\tau_z s} + e^k_{36} N^{(n3)}_{j,x} W^k_{in3} J^{k\tau_z s} + e^k_{24} N^{(n2)}_{j} W^k_{i_y n2} J^{k\tau s_z} + e^k_{14} N^{(n2)}_{j} W^k_{i_x n2} J^{k\tau s_z}$$

$$K^{k\tau s}_{\Phi u_{43}} = e^k_{33} W^k_{ij} J^{k\tau_z s_z} + e^k_{24} N^{(n2)}_{j,y} W^k_{i_y n2} J^{k\tau s} + e^k_{14} N^{(n2)}_{j,y} W^k_{i_x n2} J^{k\tau s} + e^k_{25} N^{(n1)}_{j,x} W^k_{i_y n1} J^{k\tau s} + e^k_{15} N^{(n1)}_{j,x} W^k_{i,x n1} J^{k\tau s}$$

$$K^{k\tau s}_{\Phi\Phi_{44}} = - \varepsilon^k_{33} W^k_{ij} J^{k\tau_z s_z} - \varepsilon^k_{22} W^k_{i_y j_y} J^{k\tau s} - \varepsilon^k_{12} W^k_{i_x j_y} J^{k\tau s} - \varepsilon^k_{12} W^k_{i_y j_x} J^{k\tau s} - \varepsilon^k_{11} W^k_{i_x j_x} J^{k\tau s}$$

Explicit form of mass fundamental nucleus

The mass fundamental nucleus $\boldsymbol{M}^{k\tau sij}$ is:

$$\boldsymbol{M}^{k\tau sij} = \begin{bmatrix} M_{11} & 0 & 0 & 0 \\ 0 & M_{22} & 0 & 0 \\ 0 & 0 & M_{33} & 0 \\ 0 & 0 & 0 & 0 \end{bmatrix}^{k\tau sij}$$

The elements of the nucleus are:

$$M_{11}{}^{k\tau sij} = M_{22}{}^{k\tau sij} = M_{33}{}^{k\tau sij} = \rho W^k_{ij} J^k_{\tau s}$$